Partitioning of Evapotranspiration Using a Stable Isotope Technique in an Arid and High Temperature Agricultural Production System

Xuefei Lu[1], Liyin L. Liang[2], Lixin Wang[1*], G. Darrel Jenerette[3], Matthew F. McCabe[4] and David A. Grantz[3]

[1]Department of Earth Sciences, Indiana University-Purdue University Indianapolis (IUPUI), IN 46202

[2]School of Science, University of Waikato, Hamilton, New Zealand

[3] Department of Botany & Plant Sciences, University of California Riverside, Riverside, CA 92521

[4] Water Desalination and Reuse Center, Division of Biological and Environmental Sciences and Engineering, King Abdullah University of Science and Technology, Thuwal, Saudi Arabia

*Corresponding author

Lixin Wang

Department of Earth Sciences

Indiana University-Purdue University Indianapolis

Indianapolis, IN, 46202, USA

Office phone number: 317-274-7764

Email: lxwang@iupui.edu

This is the author's manuscript of the article published in final edited form as:

Lu, X., Liang, L. L., Wang, L., Jenerette, G. D., McCabe, M. F., & Grantz, D. A. (2017). Partitioning of evapotranspiration using a stable isotope technique in an arid and high temperature agricultural production system. Agricultural Water Management, 179, 103–109. https://doi.org/10.1016/j.agwat.2016.08.012

ABSTRACT

Agricultural production in the hot and arid low desert systems of southern California relies heavily on irrigation. A better understanding of how much and to what extent irrigated water is transpired by crops relative to being lost through evaporation would improve the management of increasingly limited water resources. In this study, we examined the partitioning of evapotranspiration (ET) over a field of forage sorghum (*Sorghum bicolor*), which was under evaluation as a potential biofuel feedstock, based on isotope measurements of three irrigation cycles at the vegetative stage. This study employed customized transparent chambers coupled with a laser-based isotope analyzer to continuously measure near-surface variations in the stable isotopic composition of evaporation (E, δ_E), transpiration (T, δ_T) and ET (δ_{ET}) to partition the total water flux. Due to the extreme heat and aridity, δ_E and δ_T were very similar, which makes this system highly unusual. Contrary to an expectation that the isotopic signatures of T, E, and ET would become increasingly enriched as soils became drier, our results showed an interesting pattern that δ_E, δ_T, and δ_{ET} increased initially as soil water was depleted following irrigation, but decreased with further soil drying in mid to late irrigation cycle. These changes are likely caused by root water transport from deeper to shallower soil layers. Results indicate that about 46% of the irrigated water delivered to the crop was used as transpiration, with 54% lost as direct evaporation. This implies that 28 - 39% of the total source water was used by the crop, considering the typical 60 - 85% efficiency of flood irrigation. The stable isotope technique provided an effective means of determining surface partitioning of irrigation water in this unusually harsh production environment. The results suggest the potential to further minimize unproductive water losses in these production systems.

Keywords: Biofuel, climate change, drought, ecohydrology, El Centro, Imperial Valley, irrigation, water resources, water use efficiency.

1 Introduction

Agriculture is the largest single user of fresh water globally, accounting for approximately 70% of the total withdrawn for human consumption (Hoekstra and Mekonnen, 2012; Wada et al., 2014). In the United States (US), irrigated agriculture is the second largest primary user of fresh water, accounting for 31% of the developed water resource (Vörösmarty et al., 2000). The Imperial Valley, in the low elevation desert of southern California, a region characterized by extreme heat and evaporation, has been considered a promising area for biofuel feedstock production (Oikawa et al., 2015). This area produces more than two-thirds of winter vegetables consumed in the US and about three-quarters of summer hay and other field crops in southern California (Medellín-Azuara et al., 2012). At present, there is a lack of data addressing the sustainability, including water use efficiency, of biofuel production in this high temperature agricultural site.

The Colorado River is a key source of water for California's irrigated desert agriculture, accounting for approximately one-third of annual flow (Cohen et al., 2013). A growing demand for water, coupled with the limited supplies and impacts of climate change (Vörösmarty et al., 2000), have placed enormous pressures on California's water supply. Recent years of drought have exacerbated this water scarcity challenge, especially in the Imperial Valley.

Evapotranspiration (ET) represents one of the largest components of the global water cycle, with approximately 65% of precipitation returned to the atmosphere via ET at the global scale (Trenberth et al., 2007). However, ET loss can reach up to 95% in some dryland systems (Wang et al., 2014; Wilcox and Thurow, 2006). Evapotranspiration consists of two distinct components: evaporation from soil and plant surfaces (E) and transpiration taken up by roots and lost through stomatal pores (T). These two components are controlled by different processes and have different water use implications. Transpiration is controlled by atmospheric evaporative demand and modified by plant physiological controls on leaf stomata. Because photosynthetic carbon dioxide fixation is concurrent with water vapor loss, and shares the stomatal diffusion pathway, irrigated water transpired by crops is productive in that it facilitates photosynthesis and leads to leaf cooling. Evaporation from soil, in contrast, is not directly linked to biological processes, but rather results from diffusion of water through the soil matrix and evaporation at the surface, and is controlled solely by physical factors. Although it may lead to local evaporative cooling, this water loss is not directly linked to biological productivity. Because of the different controlling mechanisms, E and T are likely to have different responses to environmental drivers such as temperature and soil water content (Kool et al., 2014; Wang et al., 2014). As competition for available irrigation water increases, a better understanding of how much is transpired relative to that lost through evaporation, and the factors controlling this partitioning, could contribute to improved water resource management (Wang and D'Odorico, 2008).

Separating E and T has proven to be difficult. Various methods have been proposed, including empirical measurements and modeling-based approaches. Empirical measurements can include lysimeters, large tree potometers, whole tree chambers, eddy covariance measurements of above- and below-canopy fluxes, up-scaling of sap-flow measurements, and flux-variance similarity partitioning, as well as using stable isotopes (Kool et al., 2014). Modeling approaches include the FAO-56 dual crop coefficient model

(Ding et al., 2013), modeling of canopy and subcanopy fluxes driven by energy balance measurements (Ershadi et al., 2014; Kalma et al., 2008) or combining process-based modeling and isotope tracer measurements (Cai et al., 2015; Wang et al., 2015). The recent development of techniques using stable isotopes of water have provided a useful tool to separate E and T, that can be applied across broad spatial and temporal scales. Besides facilitating ET partitioning, the stable isotopic composition of E and T can also provide insights regarding plant water use dynamics as well as the nature of land-atmosphere interactions (Parkes et al., 2016).

The basis for using the isotopes of H and O in water to partition ET is that evaporation significantly fractionates the surface soil water, enriching the source with the heavier isotopes, while transpiration does not lead to fractionation when T is large (Wang et al., 2012; Wang et al., 2013). Therefore, the isotopic composition of transpiration (δ_T) remains similar to the isotopic composition of the plant source water, while the isotopic composition of evaporated water differs from that of the source. This results in distinct isotopic signatures of δ_E and δ_T (Wang et al., 2013; Zhang et al., 2011).

The development of field-deployable laser-based instruments with similar precision to traditional isotope ratio mass spectrometers (e.g., Wang et al., 2009), has provided a promising tool to separate T from E in agricultural systems (Wang et al., 2012; Wang et al., 2013). The application of such methods to direct measurement of the isotopic composition of E, T and the combination, ET, in a hot, arid agricultural production system has not previously been attempted.

The objectives of the current study are to: (1) use a laser-based isotope analyzer and customized E and ET chambers to measure the respective isotope signatures, δ_T, $\delta_{E,}$ and

δ_{ET}; (2) combine the estimates of δ_T, δ_E, δ_{ET} and total ET to partition the evaporative flux and to quantify the fraction of irrigation that is partitioned to productive T in this sorghum production system. These measurements provide important information for regional water issues, for crop management scenarios, and offer substantial insight into currently temperate production systems that may become warmer.

2 Materials and Methods

2.1 Study site

The study was conducted at the University of California's Desert Research and Extension Center (DREC) located in the Imperial Valley, southern California (32.867°N 115.448°W) (Fig. 1a). This area is an interior desert valley about 18.3 m below sea level. The weather represents a desert climate with over 350 days of sunshine. The nearest automatic weather station (Meloland, 32.806°N 115.446°W) is managed by the California Management Information System (CIMIS) (http://www.cimis.water.ca.gov). Routine meteorological variables, including solar radiation, wind, humidity, air temperature, precipitation and soil temperature, as well as reference ET (ET_o), have been recorded hourly since December 1989. The mean annual precipitation from 1990 to 2015 was 80.3 mm year^{-1}, while the mean annual ET_o reaches 1846 mm year^{-1} (Fig. 1b). Most of the rainfall occurs in late summer, with June being the driest month (Fig.1b). The mean annual temperature is 22.4°C with a monthly mean temperature of 12.6°C in January and 32.9°C in August (for the period 1990 – 2015) (Fig. 1c). The mean annual relative humidity of the study area is around 46% (Fig. 1d). The experimental field has been used for agricultural production since the establishment of DREC in 1912. Irrigation water is supplied through the All-American Canal, distributed by gravity from the

Colorado River. Irrigation is provided by regularly scheduled flooding of furrows. Soils in the regions are moderately to well-drained deep alluvial soils (42% clay, 41% silt 16% sand) with sub-surface drainage tile, and pH of 8.3.

The *Sorghum bicolor* (cv. Photoperiod LS; Scott Seed Inc.) was planted in February 2012 for biofuel production, and was cut three times each year at the end of the vegetative stage. Ten extensive field measurements of δ_T, δ_E and δ_{ET} were conducted on July 24, 26, 28, 30 and August 4, 6, 7, 13, 18 and 20, 2014. Measurements covered the three irrigation cycles of one of the three vegetative harvests obtained each year. Plants were harvested for biomass before substantial flowering had occurred, and thus remained in the vegetative stage throughout the experiment. The irrigation events occurred on July 22, July 31 and August 9, 2014, each lasting 24 hours. Isotope sampling was conducted one full day after irrigation to allow for drainage. There were two minor rainfall events during the measurement period, with a total rainfall of 1.27 mm. The mean monthly air temperature was 33.5°C and 31.9°C in July and August 2014.

2.2 Isotope-based partitioning

The technique developed by Wang et al. (2012; 2013) was modified to fit our specific needs. The isotopic compositions of the three component vapor fluxes (δ_T, δ_E and δ_{ET}) were directly quantified using a field deployable Triple Water Vapor Isotope Analyzer (T-WVIA, Los Gatos Research, Inc., Mountain View, CA, USA). Samples were obtained using customized transparent acrylic chambers containing circulation fans and directly linked as a closed system with the T-WVIA. δ_T was measured at 1 Hz with a customized leaf chamber (2 × 4 × 12 cm) having leaves sealed inside the chamber for 1 to 2 min. The δ_E and δ_{ET} were measured using a larger customized chamber (50 × 50 × 50 cm) placed over bare soil or over areas with both soil and vegetation. Chamber measurements were obtained under sunny conditions between 11:00 and 14:00 when stomata were as open as soil moisture allowed. This method has been shown to capture the short-term variations in δ_T, δ_E and δ_{ET}, including fast δ_T responses to radiation (Wang et al., 2012).

The fraction of ET partitioned to T is found through measurement of isotopic signatures δ_E, δ_T and δ_{ET}. Assuming a two-component mixing model, the transpired fraction of ET is given by:

$$\frac{T}{ET} = \frac{{}_{ET} \qquad {}_{E}}{{}_{T} \qquad {}_{E}}, \tag{1}$$

where δ_E, δ_{ET}, and δ_T are the isotope signatures of E, ET and T, respectively (Wang et al., 2010).

Keeling plot and mass balance approaches have been used to estimate the isotopic composition of vapor fluxes. The Keeling plot approach assumes constant concentration and isotopic compositions of the ambient water vapor (δ_A). Source water vapor isotopic composition (e.g., δ_E, δ_T or δ_{ET}) was calculated as:

$${}_{M} = C_A\left({}_{A} \qquad {}_{S} \right) \frac{1}{C_M} \div + \; {}_{S} , \tag{2}$$

where δ_M, δ_A and δ_S are the isotopic compositions of mixed water vapor, ambient water vapor and source water vapor in ET, E or T. C_M is the mixed water vapor concentration and C_A is the ambient water vapor concentration at the measurement location (Wang et al., 2010).

The calculation of source water vapor isotopic composition using a mass balance approach was given as:

$$_{S} = \frac{C_{M} \;_{M} \quad C_{A} \;_{A}}{C_{M} \quad C_{A}} \quad , \tag{3}$$

Under our measurement conditions, the maximum concentration of water vapor before condensation occurred in August was 49,100 ppm. Measurements were terminated when water concentration approached 45,000 ppm in order to prevent condensation. The δ_E, δ_T and δ_{ET} were measured at random locations with four repeated measurements from each sampling time. Data were excluded due to instrumental malfunction and obvious data errors (e.g., the fraction of ET is greater than 1 or less than 0). ET partitioning was not possible for August 13, August 18, and August 20, as chamber-based δ_{ET} were not available. Both $\delta^{18}O$ and δD data were used to demonstrate the temporal changes in δ_E, δ_T or δ_{ET}, while only δD data were used for ET partitioning.

2.3 Total ET measurements

Total ET was monitored at 10 Hz using the eddy-covariance technique via an open-path infrared gas analyzer (IRGA) (Li7500, LI-COR, Lincoln, NE, USA) and a 3-D sonic anemometer (CSAT3, CSI, Logan, Utah, USA) (Oikawa et al., 2015). The instrument was mounted on a tower located within 10 m of the chamber measurements, at a height of 2.5 meters above the canopy. Data processing was conducted in EddyPro 5.2 (LI-COR, Lincoln, NE, USA) and followed standard flux calculations over 30 min intervals. The footprint of the tower was determined using an approximate analytical model (Hsieh et al., 2000). Evapotranspiration fluxes with 70% of the footprint exceeding the edge of the field were removed. The ET data were gap-filled following Reichstein et al. (2005).

3 Results

This study was conducted under extremely hot and arid conditions (Fig. 1). Fig. 2 shows the hydrogen and oxygen isotopes in the evaporation and transpiration waters. The δ^{18}O of transpiration water (δ_T) ranged from -6.07 to 6.99‰, with a mean value of 0.04‰ and standard deviation of 3.60‰, while δD of δ_T ranged from -89.75 to -70.44‰, with a mean value of -83.27‰ and standard deviation of 7.28‰ (Fig. 2). The least squares fitting between δD and δ^{18}O in transpiration was: $\delta D = 1.4 \times \delta^{18}O - 83.3$ ($R^2 = 0.47$, $p < 0.05$). The δ^{18}O of evaporation water (δ_E) ranged from -4.99 to 5.10‰, with a mean value of -1.35‰ and standard deviation of 3.52‰, while δD of δ_E ranged from -97.33 to -71.07‰, with a mean value of -83.48‰ and standard deviation of 8.39‰ (Fig. 2). The least squares fitting between δD and δ^{18}O in evaporation was: $\delta D = 1.5 \times \delta^{18}O - 82.0$ ($R^2 = 0.38$, $p < 0.05$). The local meteoric water line (LMWL) determined via least squares fitting of the irrigation water isotopic values was: $\delta D = 7.3 \times \delta^{18}O + 3.6$.

All δ_E values fell to the right side of the irrigation water line, revealing a strong evaporation effect on δ_E (Fig. 2). The δD–δ^{18}O regression lines for both δ_T and δ_E deviated substantially from the LMWL, producing very negative values of deuterium excess (d-excess: defined as d-excess = $\delta D - 8.0 \times \delta^{18}O$) of δ_T = -83.3 and δ_E = -82.0‰. Although such negative d-excess values are not commonly seen, the values are comparable to those obtained in a recent study in one of the driest regions in China. In that study, a negative d-excess value of -85.6‰ in leaf water was reported (Zhao et al., 2014). In the present study, the slopes of the δD–δ^{18}O regression lines for δ_T and δ_E were much lower than 8.0, suggesting substantial water loss through direct evaporation and transpiration drawn from isotopically enriched soil water. Moreover, the intersections of δD–δ^{18}O regression lines for δ_T and δ_E and irrigation water line fell within the range of the isotopic compositions of irrigation waters, supporting an E and T origin from this source (Fig. 2).

In contrast to an expectation that the isotopic signatures of T, E, and ET would become increasingly enriched as soils became drier, our results present a more complex pattern. Here, the isotopic signatures of E, T and ET increased (less negative) initially as water was depleted, but then decreased at the end of each irrigation cycle (Fig. 3a and b). Both δD and δ^{18}O followed similar patterns and it was replicated in all three irrigation cycles (Fig. 3a and b).

ET partitioning was calculated using a simple 2-source model, as defined in Equation 1. It was estimated that about 46% ± 5.6% of the irrigated water was used as transpiration by crops after runoff as tailwater and drainage, while 54% was lost as direct evaporation from the soil (Table 1). Transpiration between May and October 2014 ranged from 0.59 to 6.08 mm/day, with a mean value of 3.04 mm/day (Fig. 4). Both T/ET and LAI increased as the crop developed (Fig. 5a) during the vegetation stage and the relationship between T/ET and LAI was $T/ET=0.45 \times LAI^{0.19}$ (Fig. 5b).

4 Discussion

An increasing number of studies have used the stable isotope technique to separate ET components, and predict ET partitioning changes under both agricultural and natural settings. Here we present one of the first studies testing the field application of a chamber method to directly measure isotopic composition of all three components (E, T and ET), in an extreme agricultural production environment. By using this approach, we could also predict the patterns of plant water use based on the changes of transpiration isotopic composition. Particularly we monitored the plant water use pattern at the vegetative stage. Water loss by evaporation can be much higher at the vegetative stage than the later growing stages (Wang et al., 2014), so any improvement of water management is critical at this stage.

Of particular interest was the examination of these evaporative processes under extremely hot and arid condition, with local conditions having a mean ET_o more than 20 times the mean annual precipitation. Due to the extreme heat and aridity, δ_E and δ_T were very similar, which is rarely seen in the literature and mark this system as quite unique (see Fig. 6). The small difference between δ_T and δ_E makes it challenging to accurately discriminate the isotopic compositions of these two fluxes, and ultimately to partition total ET into relative rates of E and T. Despite this complexity, our chamber method generally worked well for δ_T, δ_E, and δ_{ET} estimates, based on agreement between the Keeling plot and mass balance approaches (Appendix Fig. S1).

Our results yield interesting insights into how isotopic signatures of T, E and ET can change with depletion of water within the irrigation cycles. Contrary to an expectation that the isotopic signatures of T, E, and ET would continuously become enriched as soils became drier, we have observed that the isotopic signatures of E, T and ET increased as water was depleted, but decreased at the end of each irrigation cycle. The observed pattern of depleted isotopic signatures of T, E, and ET in mid to late irrigation cycles might be caused by lateral roots accessing water from deeper soil depths when shallow water is reduced, redistributing the deeper water to shallower layers (Ahmed et al., 2016; Stone et al., 2001). The root system of maize, a related C_4 grass, consists of pre-embryonic primary and seminal roots formed during embryogenesis and lateral roots formed during post-embryonic development (Ahmed et al., 2016). A recent study using neutron radiography to examine the mechanism of maize root water uptake has found that the function of lateral roots is to uptake water from the soil while the function of primary and seminal roots is to axially transport water to the shoot (Ahmed et al., 2016). As sorghum has similar root water uptake dynamics to corn (Srayeddin and Doussan, 2009), this rooting mechanism might explain why the isotopic signatures of E, T, and ET increase but then decrease within the irrigation cycles. As sorghum roots grow steadily throughout the season, when the shallow water is depleted and soil dries, the lateral roots could extract water from the subsoil and redistribute to the surface layer for transpiration and evaporation, leading to isotopic depletion of E, T and ET.

Other factors such as soil properties and precipitation could also influence the isotopic compositions of different components and ET amount. The small precipitation events occurring on August 2 and August 3, 2014 likely caused a higher value of δ_E on Aug 4 and 6 (Fig. 5) due to a strong evaporation of the rainfall on surface soil. The δ_T is lower than δ_E for these two cases because transpiration response is likely damped due to the crop water use from deeper soil layers, in addition to the use of limited surface rainfall water. The daily average soil moisture varies between 0.17 and 0.42 $cm^3\ cm^{-3}$ (Oikawa et al., 2014), and all samplings were conducted after irrigation when the field is still at field capacity.

Transpiration values measured at our site were comparable to those measured in other dryland agriculture sites. However, the ratio of transpiration to evapotranspiration (T/ET) was considerably lower. For example, a study in China found that the measured T ranged from 1.02 to 4.91 mm/day, accounting for 60% to 83% of the total ET (Zhang et al., 2011). Based on this study, the ratio of transpiration to evapotranspiration (T/ET) slightly increased with the increasing trend of leaf area index (LAI) as crops develop (Fig. 5), and the relationship between T/ET and LAI from our study is in-between those reported in previous study for early season and peak LAI stage (Wang et al., 2014). We have estimated that the rate of evaporation could be as high as 54% at the vegetative stage, thus it may be possible to improve water use efficiency of sorghum at the early growing stage in such systems with extremely limited water resources. The vegetative stage may play a dominant role in seasonal T/ET (Kang et al., 2003; Wang et al., 2014), particularly in forage and lignocellulosic biofuel systems which remain in the vegetative stage. Our measurements from one vegetative harvest cycle may be representative of the water use dynamics of the entire growing season.

Like many crops in the Imperial Valley, the forage sorghum evaluated here was irrigated through flooding of furrows. Compared to the other irrigation systems such as drip and spray irrigation, flood irrigation exhibits some inefficiencies due to surface runoff, deep percolation and unproductive evaporative losses (Cooley et al., 2009). However, flood systems have advantages such as simplicity of design, low capital investment, and low energy requirement. Deep drainage to the tile system is critical in this environment to leach salts that are accumulated from the irrigation water (Oikawa et al., 2015). The Colorado River, at the point of interception of the All American Canal, has a salinity of 879 mg L^{-1} TDS (Forum, 2011).

It has been estimated that the potential irrigation efficiency (defined as the volume of water used by the plant divided by the volume of irrigation water applied to the field minus changes in surface and soil storage) for flood irrigation systems ranges from 60 – 85% (Cooley et al., 2009). Combining the current analysis and the typical efficiency of flood irrigation system, the amount of water used by the plant via transpiration relative to the amount of water delivered to the field in this case ranged from 28 - 39%. This indicates that although the production of biofuel feedstock is extremely high under the climate and soil conditions of this region (Oikawa et al., 2015), the water use and water use efficiency may need to be taken into consideration for the sake of sustainability.

5 Conclusions

This study presents a novel application of the combined use of customized chambers and a laser-based isotope analyzer to directly quantify isotopic signatures of T, E and ET *in situ* and examine ET partitioning over a field of forage sorghum in an extreme field condition. As a consequence of strong evaporation under extreme heat and arid conditions, the studied system showed similar δ_T and δ_E values, which is rarely seen in the literature and increases the difficulty in discriminating isotopic signatures and to partition ET. The strong evaporative gradient in this ecosystem was supported by the fact of very low slopes of δD and $\delta^{18}O$ relationship for both δ_T and δ_E.

The results revealed an interesting pattern of the isotopic signatures of E, T, and ET. All components increased as the soil dried, but decreased at the mid to end of each irrigation cycle. These changes were likely a result of the lateral roots extracting water from the subsoil and redistribution to the surface layer, so both crop and surface soil evaporation would access water from deeper layers when the shallow water is depleted.

For the studied ecosystem, approximately 46% of the irrigated water delivered to the crops was transpired, with 54% was lost via direct evaporation from the soil during the vegetative stage. Considering inherent irrigation inefficiencies, approximately 28 - 39%

of the total source water was used by crops, suggesting potential for improved water use efficiency.

Acknowledgements

We acknowledge the support by USDA-NIFA Award No. 2011-67009-30045 and partial support from the U.S. National Science Foundation (IIA-1427642 and EAR-155489). Matthew McCabe was supported by funding from the King Abdullah University of Science and Technology. We thank Dr. Yucui Zhang and one anonymous reviewer for their valuable comments, which greatly improved the quality of the manuscript.

References

Ahmed, M.A., Zarebanadkouki, M., Kroener, E., Kaestner, A., Carminati, A., 2016. Measurements of water uptake of maize roots: the key function of lateral roots. Plant Soil 398, 59-77.

Cai, M.Y., Wang, L., Parkes, S.D., Strauss, J., McCabe, M.F., Evans, J.P., Griffiths, A.D., 2015. Stable water isotope and surface heat flux simulation using ISOLSM: evaluation against in-situ measurements. Journal of Hydrology 523, 67-78.

Cohen, M., Christian-Smith, J., Berggren, J., 2013. Water to Supply the Land.

Cooley, H., Christian-Smith, J., Gleick, P.H., 2009. Sustaining California agriculture in an uncertain future.

Ding, R., Kang, S., Zhang, Y., Hao, X., Tong, L., Du, T., 2013. Partitioning evapotranspiration into soil evaporation and transpiration using a modified dual crop coefficient model in irrigated maize field with ground-mulching. Agricultural water management 127, 85-96.

Ershadi, A., McCabe, M.F., Evans, J.P., Chaney, N.W., Wood, E.F., 2014. Multi-site evaluation of terrestrial evaporation models using FLUXNET data. Agric. For. Meteorol. 187, 46-61.

Forum, C.R.B.S.C., 2011. Water Quality Standards for Salinity Colorado River System
Hoekstra, A.Y., Mekonnen, M.M., 2012. The water footprint of humanity. Proceedings of the national academy of sciences 109, 3232-3237.

Hsieh, C.I., Katul, G., Chi, T.W., 2000. An approximate analytical model for footprint estimation of scalar fluxes in thermally stratified atmospheric flows. Advances in Water Resources 23, 765-772.

Kalma, J., McVicar, T., McCabe, M., 2008. Estimating land surface evaporation: A review of methods using remotely sensed surface temperature data. Surveys in Geophysics 29, 421-469.

Kang, S., Gu, B., Du, T., Zhang, J., 2003. Crop coefficient and ratio of transpiration to evapotranspiration of winter wheat and maize in a semi-humid region. Agricultural water management 59, 239-254.

Kool, D., Agam, N., Lazarovitch, N., Heitman, J.L., Sauer, T.J., Ben-Gal, A., 2014. A review of approaches for evapotranspiration partitioning. Agric. For. Meteorol. 184, 56-70.

Medellín-Azuara, J., Vergati, J.A., Sumner, D.A., Howitt, R.E., Lund, J.R., 2012. Analysis of effects of reduced supply of water on agricultural production and irrigation water use in Southern California.

Oikawa, P.Y., Gratz, D.A., Chatterjee, A., Eberwein, J.E., Allsman, L.A., Jenerette, G.D., 2014. Unifying soil respiration pulses, inhibition, and temperature hysteresis through dynamics of labile carbon and soil O2. J. Geophys. Res.-Biogeo 115, 521-536.

Oikawa, P.Y., Jenerette, G.D., Grantz, D.A., 2015. Offsetting high water demands with high productivity: Sorghum as a biofuel crop in a high irradiance arid ecosystem. GCB Bioenergy 7, 974-983.

Parkes, S.D., McCabe, M.F., Griffiths, A.D., Wang, L., Chambers, S., Ershadi, A., Williams, A.G., Strauss, J., Element, A., 2016. Response of water vapour D-excess to land-atmosphere interactions in a semi-arid environment. Hydrol. Earth Syst. Sci. Discuss.

Reichstein, M., Falge, E., Baldocchi, D., Papale, D., Aubinet, M., Berbigier, P., Grünwald, T., 2005. On the separation of net ecosystem exchange into assimilation and ecosystem respiration: review and improved algorithm. Glob. Change Biol. 11, 1424-1439.

Srayeddin, I., Doussan, C., 2009. Estimation of the spatial variability of root water uptake of maize and sorghum at the field scale by electrical resistivity tomography. Plant Soil 319, 185-207.

Stone, L.R., Goodrum, D.E., Jaafar, M.N., Khan, A.H., 2001. Rooting front and water depletion depths in grain sorghum and sunflower. Agronomy Journal 93, 1105-1110.

Trenberth, K.E., Smith, L., Qian, T., Dai, A., Fasullo, J., 2007. Estimates of the global water budget and its annual cycle using observational and model data. Journal of Hydrometeorology 8, 758–769.

Vörösmarty, C.J., Green, P., Salisbury, J., Lammers, R.B., 2000. Global water resources: vulnerability from climate change and population growth. Science 289, 284-288.

Wada, Y., Wisser, D., Bierkens, M.F.P., 2014. Global modeling of withdrawal, allocation and consumptive use of surface water and groundwater resources. Earth System Dynamics 5, 15-40.

Wang, L., Caylor, K., Dragoni, D., 2009. On the calibration of continuous, high-precision $\delta^{18}O$ and $\delta^{2}H$ measurements using an off-axis integrated cavity output spectrometer Rapid Communications in Mass Spectrometry 23, 530-536.

Wang, L., Caylor, K.K., Villegas, J.C., Barron-Gafford, G.A., Breshears, D.D., Huxman, T.E., 2010. Evapotranspiration partitioning with woody plant cover: assessment of a stable isotope technique. Geophysical Research Letters 37, L09401.

Wang, L., D'Odorico, P., 2008. The limits of water pumps. Science 321, 36-37.

Wang, L., Good, S.P., Caylor, K.K., 2014. Global synthesis of vegetation control on evapotranspiration partitioning. Geophysical Research Letters 41, 6753–6757.

Wang, L., Good, S.P., Caylor, K.K., Cernusak, L.A., 2012. Direct quantification of leaf transpiration isotopic composition. Agric. For. Meteorol. 154-155, 127-135.

Wang, L., Niu, S., Good, S., Soderberg, K., Zhou, X., Xia, J., Sherry, R., Luo, Y., Caylor, K., McCabe, M., 2013. The effect of warming on grassland evapotranspiration partitioning using laser-based isotope monitoring techniques. Geochimica et Cosmochimica Acta 111, 28-38.

Wang, P., Yamanaka, T., Li, X.Y., Wei, Z., 2015. Partitioning evapotranspiration in a temperate grassland ecosystem: Numerical modeling with isotopic tracers. Agric. For. Meteorol. 208, 16-31.

Wilcox, B.P., Thurow, T.L., 2006. Emerging issues in rangeland ecohydrology: vegetation change and the water cycle. Rangeland Ecology & Management 59, 220–224.

Zhang, Y., Shen, Y., Sun, H., Gates, J.B., 2011. Evapotranspiration and its partitioning in an irrigated winter wheat field: A combined isotopic and micrometeorologic approach. Journal of Hydrology 408, 203-211.

Zhao, L., Wang, L., Liu, X., Xiao, H., Ruan, Y., Zhou, M., 2014. The patterns and implications of diurnal variations in the d-excess of plant water, shallow soil water and air moisture. Hydrology and Earth System Sciences 18, 4129-4151.

Table 1. Evapotranspiration partitioning calculations at representative sampling dates.

Date	**%T**	**%E**
7/24/2014	40.2	59.8
7/28/2014	39.3	60.7
7/30/2014	51.8	48.2
8/4/2014	47.3	52.7
8/6/2014	52.3	47.7
8/7/2014	45.0	55.0
Mean	**46.0**	**54.0**
SD	**5.6**	**5.6**

Note: SD refers to standard deviation.

Figure Legends

Figure 1. Location of the University of California Desert Research and Extension Center (DREC). Monthly mean precipitation (mm), reference evapotranspiration (ET_o) (mm), temperature and relative humidity over 1990 – 2015 for the Meloland station of the California Irrigation Management Information System (CIMIS), located within a few hundred meters of the experimental field.

Figure 2. The δD-$\delta^{18}O$ relationships of leaf transpiration (δ_T, blue circles) and soil evaporation (δ_E, red circles). Black circles depict the measured isotopic composition of the irrigation water. The dashed black line is the Local Meteoric Water Line, determined via least-squares fitting of the irrigated water isotope values. The solid gray line is the Global Meteoric Water Line (GMWL). VSMOW is Vienna Standard Mean Ocean Water.

Figure 3. Patterns of deuterium and oxygen isotope signatures for transpiration (T), evaporation (E) and evapotranspiration (ET) over the three irrigation cycles. (a) observed pattern for deuterium (δD), (b) observed pattern for oxygen ($\delta^{18}O$). VSMOW stands for Vienna Standard Mean Ocean Water.

Figure 4. Daily variation of transpiration (T) and evapotranspiration (ET) during the vegetative stage, calculated by combing isotope partitioning and total ET results obtained from concurrent eddy covariance measurements.

Figure 5. Variations of leaf area index (LAI) during crop development (a) and the relationship between T/ET and LAI (b).

Figure 6. Comparison of deuterium isotope signature of leaf transpiration (δ_T) and soil evaporation (δ_E) over the measurement period. VSMOW stands for Vienna Standard Mean Ocean Water.

Figures

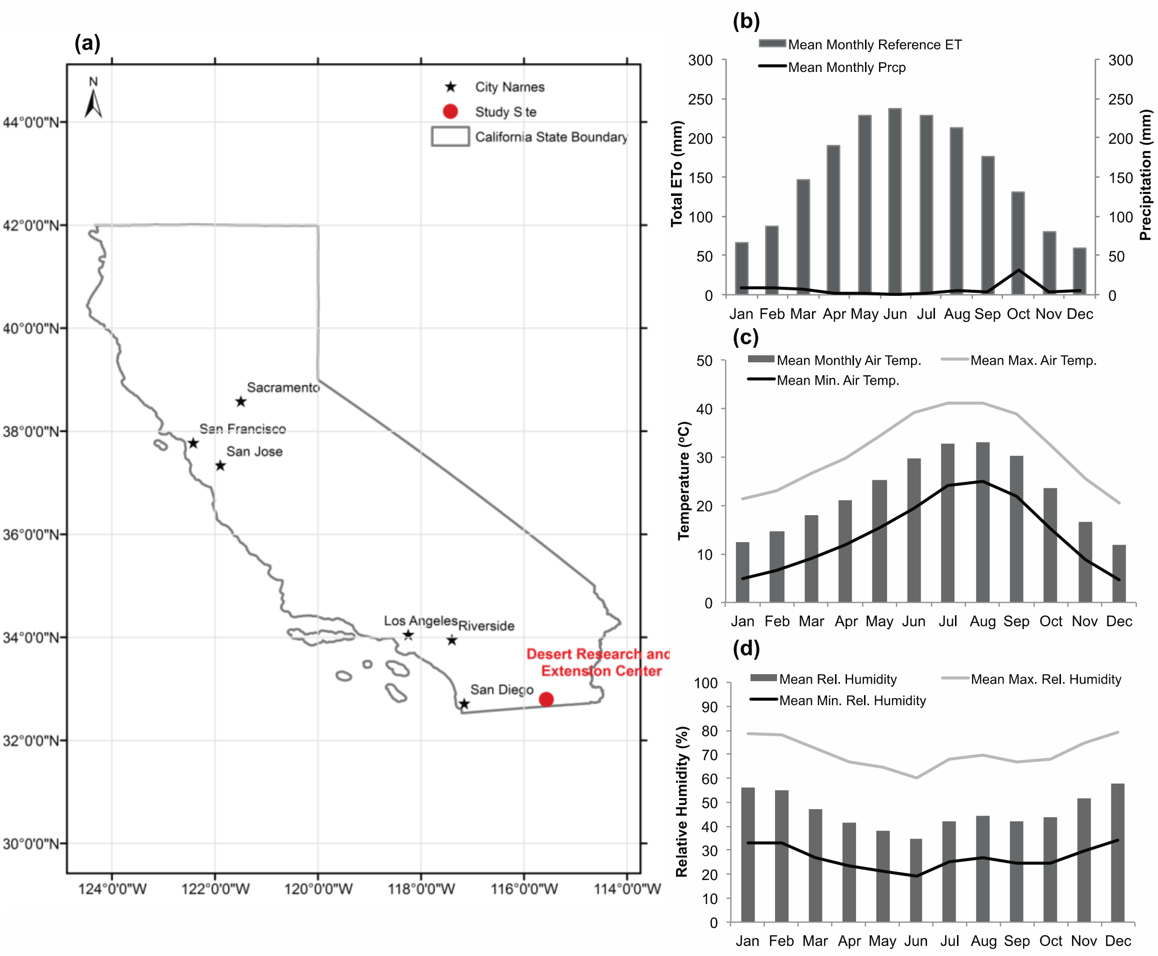

Figure 1

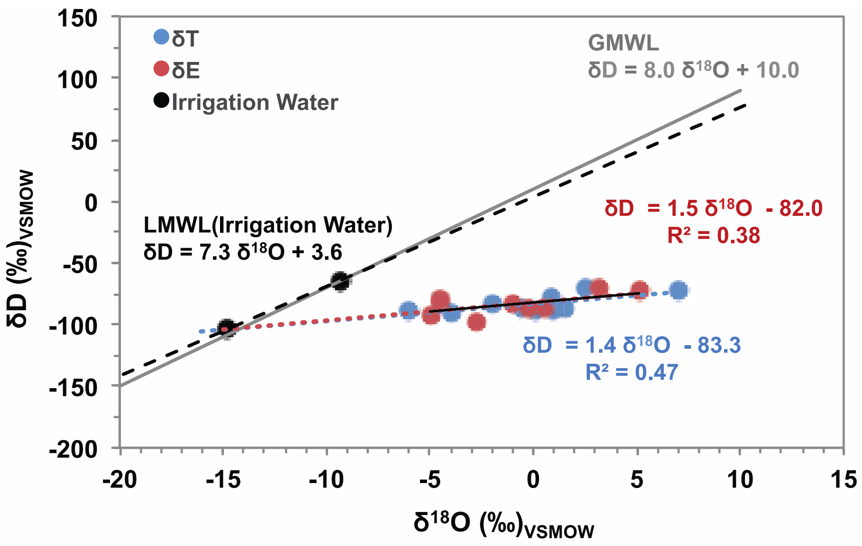
δT
δE
Irrigation Water
GMWL
δD = 8.0 δ18O + 10.0
LMWL(Irrigation Water)
δD = 7.3 δ18O + 3.6
δD = 1.5 δ18O - 82.0
R² = 0.38
δD = 1.4 δ18O - 83.3
R² = 0.47
δD (‰)VSMOW
δ18O (‰)VSMOW
150
100
50
0
-50
-100
-150
-200
-20
-15
-10
-5
0
5
10
15

Figure 2

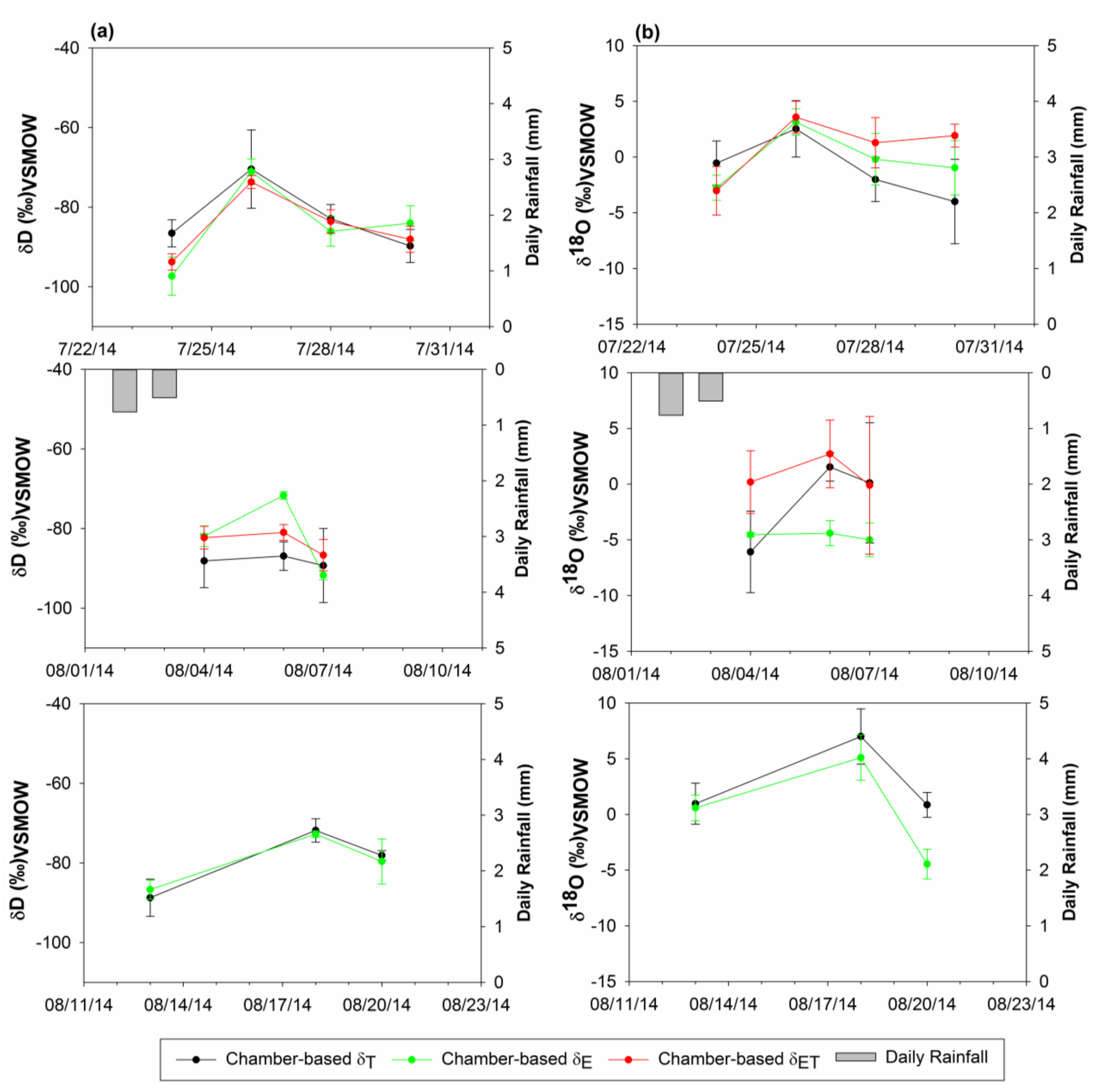
(a)
(b)
δD (‰)VSMOW
δ18O (‰)VSMOW
Daily Rainfall (mm)
-40
-60
-80
-100
10
5
0
-5
-10
-15
0
1
2
3
4
5
7/22/14
7/25/14
7/28/14
7/31/14
07/22/14
07/25/14
07/28/14
07/31/14
08/01/14
08/04/14
08/07/14
08/10/14
08/11/14
08/14/14
08/17/14
08/20/14
08/23/14
Chamber-based δT
Chamber-based δE
Chamber-based δET
Daily Rainfall

Figure 3

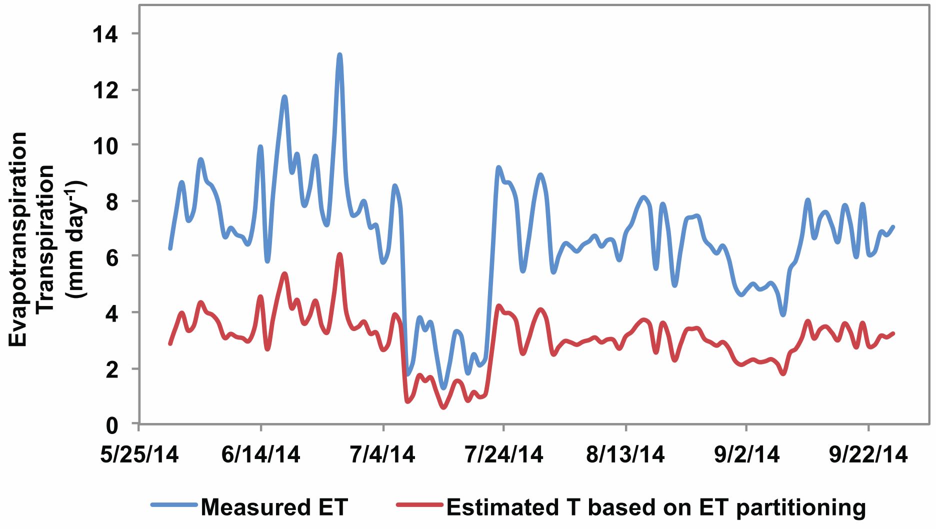
Evapotranspiration
Transpiration
(mm day^{-1})
14
12
10
8
6
4
2
0
5/25/14
6/14/14
7/4/14
7/24/14
8/13/14
9/2/14
9/22/14
Measured ET
Estimated T based on ET partitioning

Figure 4

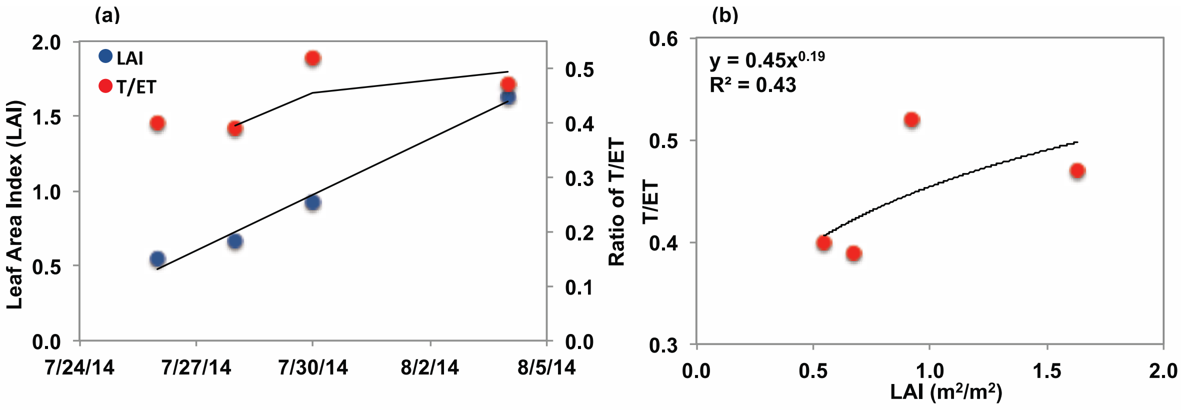
(a)
LAI
T/ET
Leaf Area Index (LAI)
Ratio of T/ET
2.0
1.5
1.0
0.5
0.0
0.5
0.4
0.3
0.2
0.1
0.0
7/24/14
7/27/14
7/30/14
8/2/14
8/5/14
(b)
y = 0.45x^0.19
R² = 0.43
T/ET
0.6
0.5
0.4
0.3
0.0
0.5
1.0
1.5
2.0
LAI (m²/m²)

Figure 5

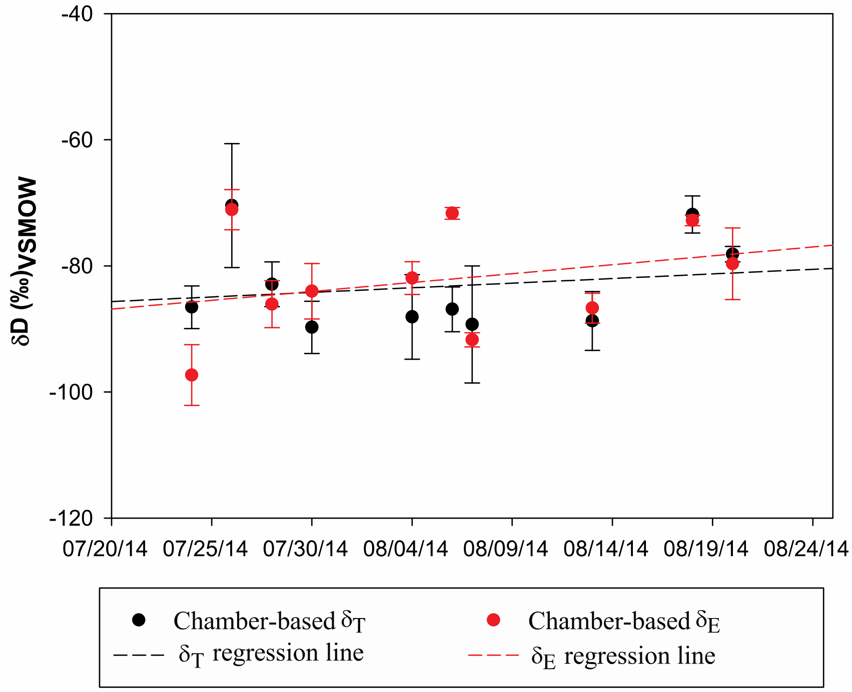
-40
-60
-80
-100
-120
δD (‰)VSMOW
07/20/14
07/25/14
07/30/14
08/04/14
08/09/14
08/14/14
08/19/14
08/24/14
● Chamber-based δ_T
● Chamber-based δ_E
δ_T regression line
δ_E regression line

Figure 6